Detection of Label-Free Biomolecules by Wavelength-Scanning Reflective Interferometric Sensing

Jinghui Lu[1,2], Tingjuan Gao[3,2] and Lewis J. Rothberg[3,1,4,2]

[1]Department of Chemical Engineering, University of Rochester, [2]Center for Future Health, University of Rochester, [3]Department of Chemistry and [4]Department of Physics, University of Rochester, Rochester, New York State, 14627

Prepared for Presentation at AIChE Annual meeting/ November 7-12/Advances in Biosensor I

Introduction

Studies in sensing of biomolecules such as DNAs, RNAs and bacterial pathogens have grown rapidly and triggered many applications in biological research. Previously reported techniques have shown great significance in the area of medical tests, environmental monitoring and medicine (Cooper, 2002). Sensitivity and selectivity of the detection have been improved by fluorescent tagging of molecules in the analyte samples (Chee et.al.,1996; Iyer et.al., 1999) but this process is expensive and time-consuming. Additionally, the detector and the imaging system that are required by the current fluorescent readout schemes are complicated and expensive. Further studies focus efforts on two aspects: avoiding modification of the analyte to simplify the chemistry and reducing the cost to make easily portable readout systems. Ellipsometric approaches (Jin et.al.,1995; Landry & Zhu, 2004), Interferometric methods (Lin et.al.,1997; Jenison et.al.,2000;Chan et.al., 2001; Pan & Rothberg,2003) and Surface Plasmon Resonance (Knoll, 1998; Nelson et.al.,2001) still require relatively complex detection systems. Simple chemistry and inexpensive detection, while maintaining the high sensitivity and selectivity, continue to be goals for developing an efficient biomolecular sensing technique.

We here describe a new chip-based method, Reflective Interferometric Sensing (RIS), which is able to detect binding of as little as 0.2-nm-thick coverage of target molecules on the sensing surface, It is quantitative, inexpensive and the molecules under investigation are label-free.

Principle

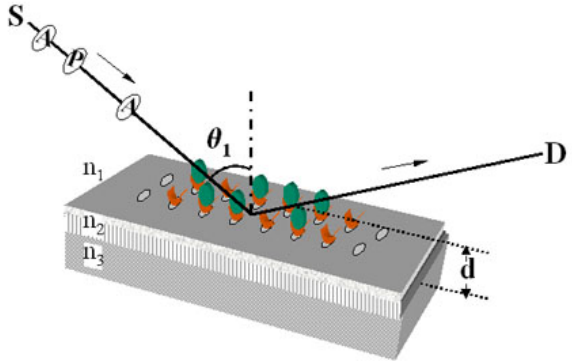

Figure 1. Schematic of the substrate composition and measurement geometry. S, A, P and D representing the optics are light source, aperture, polarizer and detector. θ_1 is the incident angle, d is the aggregate thickness of the fabricated functional layers and thermally grown SiO_2 layer (not to scale). n_1, n_2 and n_3, the refractive indices of air, the oxide/biomolecular coating and Si respectively.

Silicon with a thick thermal oxide is used as RIS substrate. Figure 1 depicts the schematic of the substrate and sensing geometry. A substrate with a coating of thickness d is surface-functionalized with probe molecules for the desired target. The reflection of TE (s-polarized) light incident at an angle θ_1 vanishes for a particular wavelength λ by destructive interference of the reflected beams at the air/oxide interface and the oxide/silicon interface. The reflectivity R_s from the structure shown in Figure 1 is simply expressed as eq.1 (Born & Wolf, 1975)

$$R_s = \left| \frac{r_{12} + r_{23} e^{-i\delta}}{1 + r_{12} r_{23} e^{-i\delta}} \right|^2 \qquad (1)$$

where $r_{ij} = (n_i \cos\theta_i - n_j \cos\theta_j)/(n_i \cos\theta_i + n_j \cos\theta_j)$ are the Fresnel reflection coefficients for the TE light at the interface between i and j. n_i and n_j are the complex refractive indices of various layers, $i=(-1)^{1/2}$, $\delta=(4\pi/\lambda)n_2 d\cos\theta_2$.

Distinct from other interferometric approaches (Jenison et.al.,2000), it is essential for RIS to choose TE light polarization to minimize the reflection. Using red probe wavelength in the visible region far below the direct band gap of silicon, the backside reflections from the substrate have been eliminated, and the imaginary part of the refractive index is negligible. The conditions of reflectivity minimum $\delta \approx \pi$ and $r_{12} \approx r_{23}$ are given by setting $R_s=0$, and easily solved to obtain the optimal incident angle θ_1 and oxide coating thickness d.

$$\theta_1 = \arcsin\left(\frac{n_3^2 - n_2^4/n_1^2}{n_1^2 + n_3^2 - 2n_2^2}\right)^{1/2} \qquad (2a)$$

$$H = \frac{d}{\lambda} = \frac{1}{4}\left(n_2^2 - n_1^2 \sin^2\theta_1\right)^{-1/2} \qquad (2b)$$

for the air/SiO_2/Si structure depicted in Figure 1, when $n_1=1$, $n_2=1.4563$ and $n_3=3.8251$, the theory predicts optimal incident angle $\theta_1=70.6^o$ and H=0.2253, as shown in Figure 2.

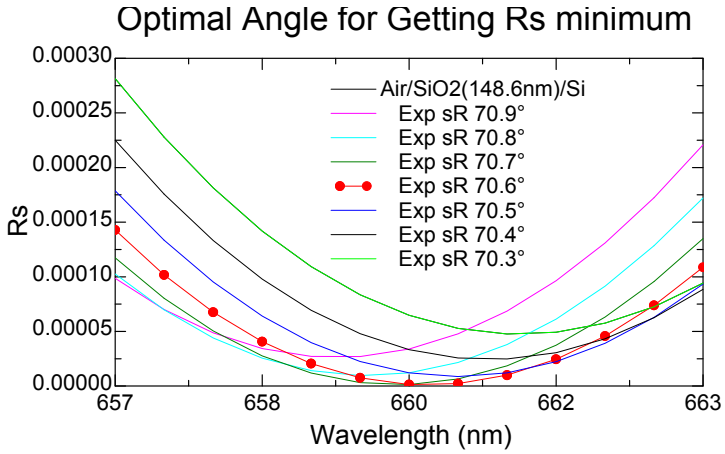

Figure 2. Modeling of optimal incident angle for the structure of Air/SiO_2(148.6nm)/Si. Reflectivity minimum value increases as the incident angle is chosen further from the optimal angle 70.6°

The reflectivity change resulting from surface thickness change is modeled in Figure 3. Upon binding with the target molecules to the probes, the reflectivity at the original wavelength

(e.g. 660nm) increases or, in other words, the wavelength at which destructive interference occurs shifts to the red (e.g. 670nm), a 1nm shift corresponding to each 0.225nm change in the coating thickness. The contrast at different regions of the surface or from before and after binding is easily detectable using RIS.

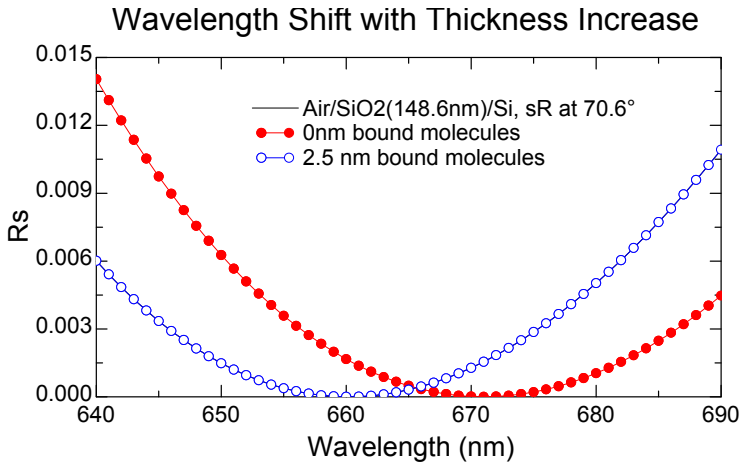

Figure 3. Theoretical illustration of the relation between the surface thickness and the wavelength at which the reflection of TE light vanishes for destructive interference. Blue line represents the region without bound molecules, and red line stands for the region with bound molecules of about 2.5nm.

Experiments and Discussion

In wavelength-scanning RIS, the sensing measurement of a substrate is taken in a wavelength range near the wavelength at which R_s of the scanned region has a minimum value. Such wavelength of minimum R_s can be found out by fitting the experimental data to a parabolic minimum and then used in Eq. 2b to compute the corresponding "coating" thickness d and hence the topology of the substrate surface.

The accuracy of the method is constrained by how well the reflectivity minimum can be determined and this depends on how close the optical arrangement is to the ideal geometry described above. The model we use to determine the effect of binding in Figure 3 assume that the optimal angle of the incident probe beam is perfectly collimated, that the light source and the reflected beam are extremely well monochromatized and that there is no surface roughness. We have therefore studied theoretically what happens when these assumptions are relaxed. The effect of the angular divergence of the incident beam, the finite bandwidth of the light and the surface roughness were each studied separately with the other two at ideal conditions. However, modeling all three nonideal conditions together does not substantively alter the conclusion. The substrate structure is set to be air/ SiO_2(148.6nm)/Si.

$\Delta\theta$ is used to represent angular divergence and Figure 4a shows the reflectivity R_s with as it is varied. The change in wavelength of the reflectivity minimum is unaltered by angular divergence, of course, but the ability to determine the position of the minimum is greatly degraded as the divergence increases. The reduction of the reflectivity contrast caused by angular divergence of 2° (open circle curves) was compared to that of 0° (solid circle curves) using the calculations in Figure 4b. In both cases, the wavelengths of minimum R_s red-shifted from around 660nm (blue curves) to around 664.5nm (red curves) after binding with 1nm analytes. However, the desired reflectivity contrast dropped severely with a 2° angular divergence, making it more difficult to determine the wavelength of minimum R_s. Comparison

was made under reflectivities at 660nm and 664.5nm with their nearby wavelengths, 659nm and 663.5nm respectively. When $\Delta\theta = 2°$, $R_{s(2°,659)}/ R_{s(2°,660)} \approx R_{s(2°,663.5)}/ R_{s(2°,664.5)} \approx 1.06$ so that it is necessary to determine reflectivity values to much better than 6 %. when $\Delta\theta = 0°$, $R_{s(0°,659)}/ R_{s(0°,660)} \approx R_{s(0°,663.5)}/ R_{s(0°,664.5)} \approx 800$ so that a sharp minimum is easily detected. Achieving excellent collimation of the incident beam to reduce the angular divergence is a key factor to optimize the detection sensitivity of RIS.

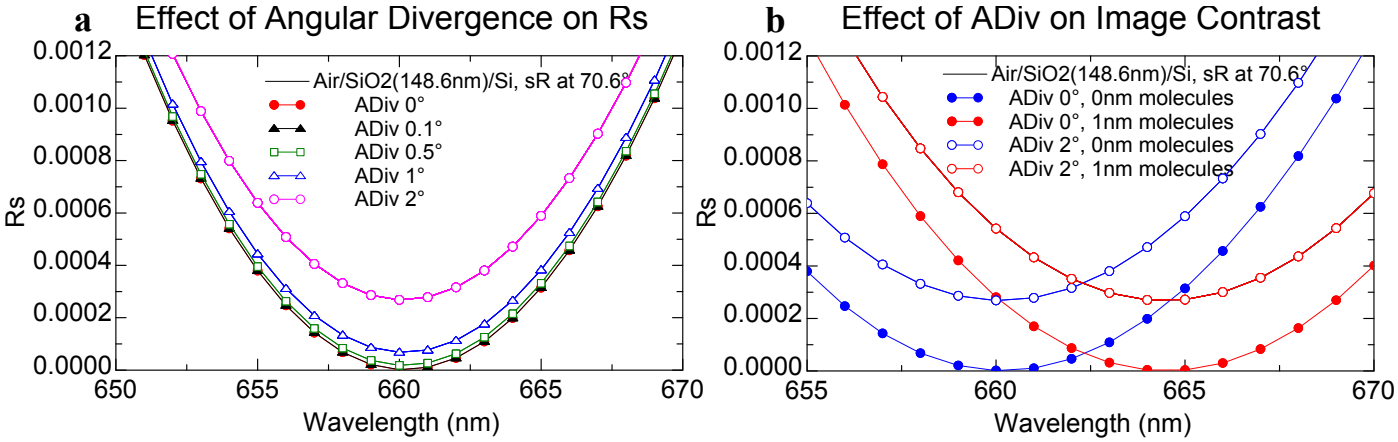

Figure 4. Effect of angular divergence on RIS. (a). Angular divergence causes increase of s-reflectivity minimum, (b). Contrast of image decreases largely with increase of angular divergence

Finite bandwidth also reduces the ability to determine reflectivity minima for the same reasons. Effect of nonmonochromaticity of the beam on the reflectivity is depicted in Figure 5. The theory predicts that this effect is smaller than the effect of angular divergence for the spectrometer slit widths and collimation that we use in our experiments.

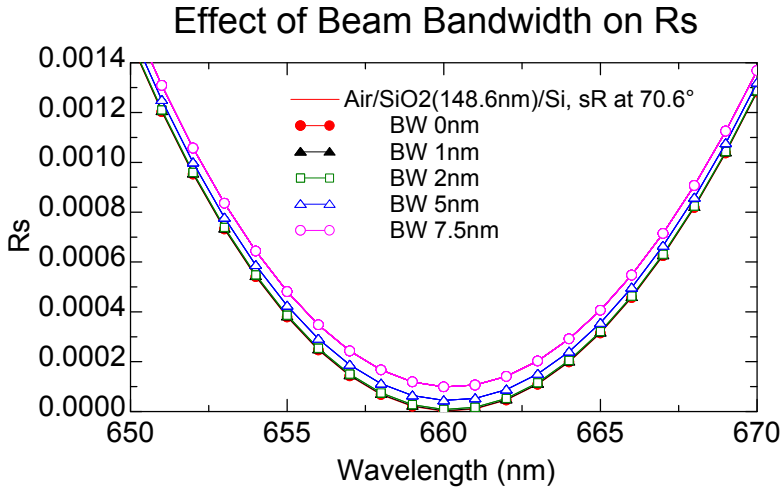

Figure 5. Effect of beam bandwidth on RIS. Rs minimum increases when bandwidth becomes bigger.

Roughness of the surface also causes degradation of the sharpness of the reflectivity minimum but modeling suggests that it tends not to be limiting for typical thermal oxides grown on silicon. The relevant roughness is also that averaged over dimensions around those of the wavelength of light. Roughness here is given by comparing the height in thickness of the rough regions from the surface with the thickness of the entire coating assembly which is about 150nm including the oxide layer and the modification layers. For instance, 1% roughness means that the top surface varies around 1.5nm in thickness. While this is much better than is

typically obtained for commercially manufactured oxides on silicon, the local variations on the size of practical sensing regions are smaller than the variation of thickness over a wafer. An experimental example is illustrated in Figure 6b which presents a cross-sectional view of a substrate surface with surface attachment layer on the oxide but prior to attaching probe biomolecules.

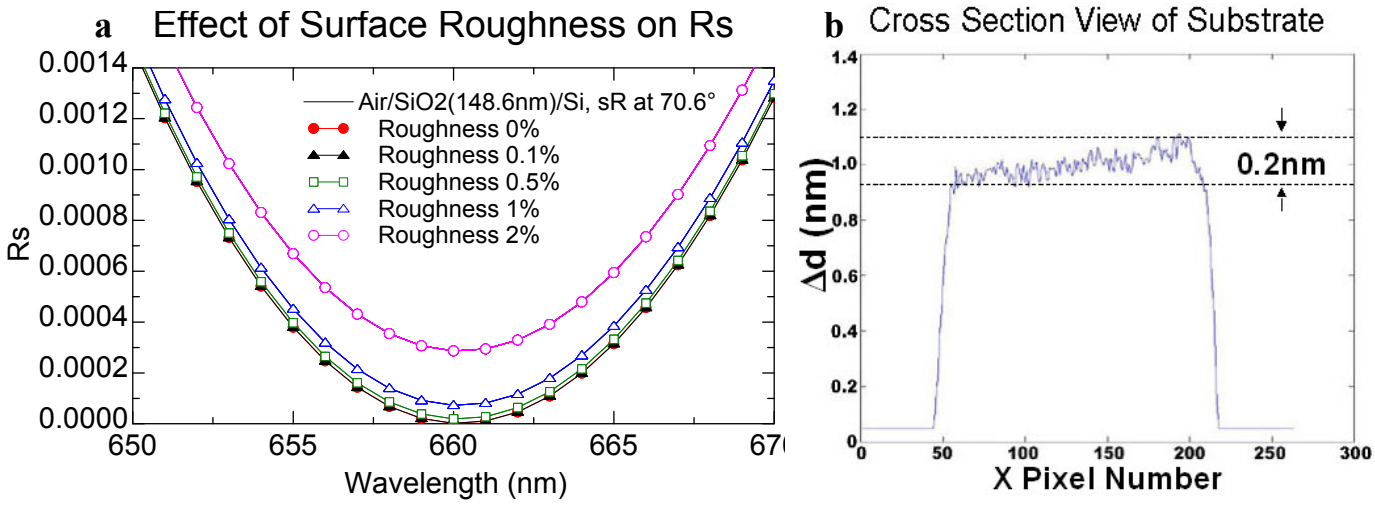

Figure 6. Effect of surface roughness on RIS. (a), Rs minimum increases when the substrate surface is getting more irregular. (b), X-cross-section view of a modified substrate surface showing the roughness, axis x is X pixel numbers and axis y is surface height in nm derived from eq 2b with further subtracting most of the oxide thickness, about 0.2nm difference in the surface height is observed.

For microarray detection, it is desirable to pattern the hydrophilicity of the substrate surface to create independent reaction wells. Crystal silicon wafers with thermally grown oxide of thickness about 150nm were diced into 1.5cm×1.5cm pieces to be used as the substrates. Cleaned in the piranha solution, the substrates were then patterned with photoresist arrays using photolithography. This was followed by silanization with octaldecyltrichlorosilane (OTS) which formed a very compact and inert hydrophobic monolayer on the bare SiO_2 surface. The photoresist arrays were washed away afterwards to expose bare SiO_2 wells separated by OTS background as illustrated in Figure 7. The functionalization chemistry was then carried out in the hydrophilic reaction wells. The pattern confines droplets containing probe and target to the wells and allows for "built-in" control experiments.

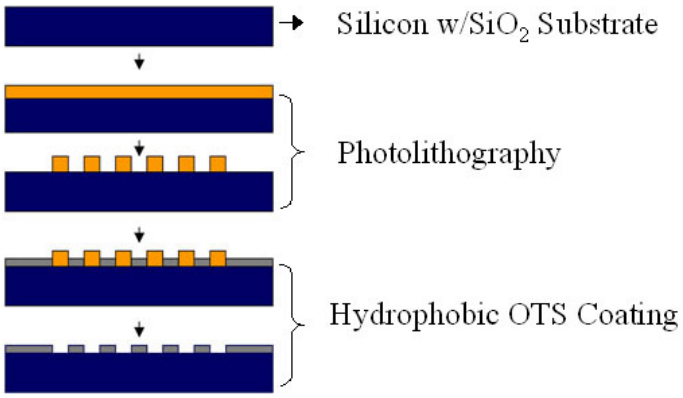

Figure 7. Hydrophilicity design of the substrate surface in microarray pattern. The yellow layer is photoresist film and the gray layer is the OTS coating.

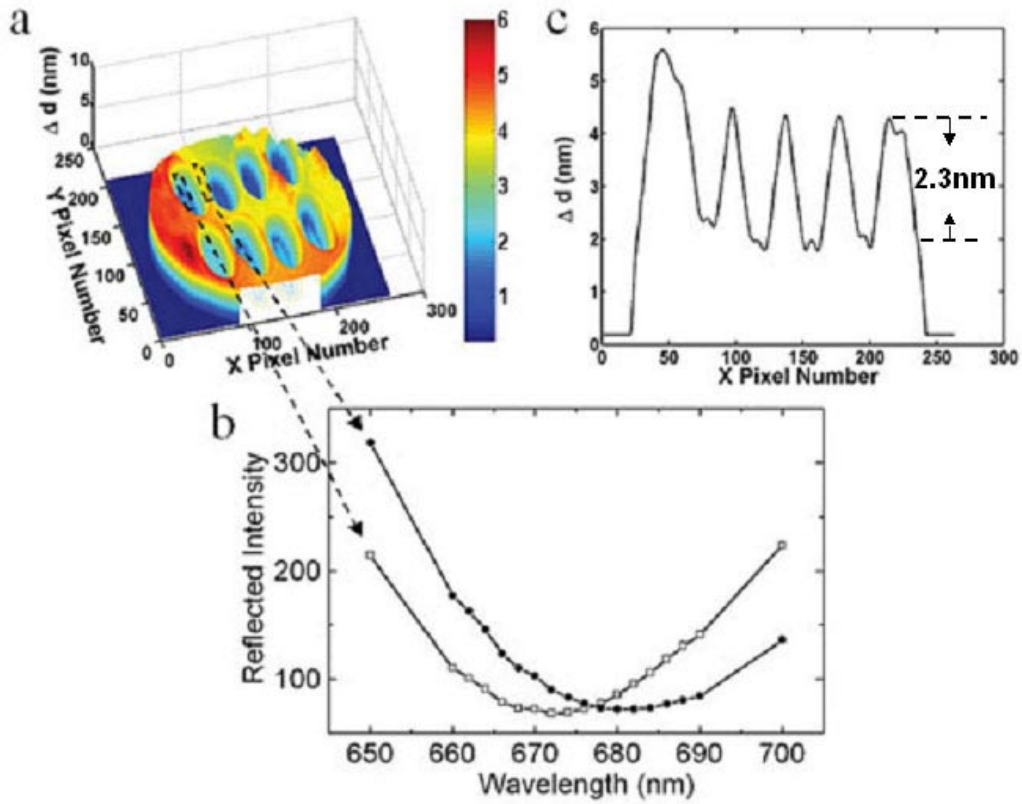

Figure 8. Surface topology of substrate with pre-arrayed bare wells. (a) 3D color map of the patterned substrate surface. The X and Y Pixel numbers derive from those of the CCD array format (1317(X)×1035(Y)) after binning regions of 5×5 from raw data to reduce to an array 263 x 207. The actual distance scale is 8.98mm×7.04mm overall with each original pixel 6.8×6.8μm. (b) Raw reflection versus wavelength derived at two different regions shown as open circles (in well) & solid circles (out of well) labeled in (a). (c) X-cross-section view of the four front wells/OTS background of the substrate surface shown in (a) where about ten Y positions have been averaged, y axis is of same meaning as in Figure 6b.

The data of figure 8 have been used to verify the concept of RIS. Reflectivity versus position for a substrate patterned with OTS as described above was measured for 18 wavelengths at angle of ~70.6^{o} using a CCD camera. A reconstruction of the surface topology using equation 2b is displayed in Figure 8a. The oval features in the circular region correspond to circular hydrophilic wells on the substrate; their aspect ratio is distorted by tan(70.6^{o}) = 2.7 due to the oblique incidence of the probe beam on the substrate. The circular region mirrors the reflected light from the OTS background. Figure 8b compared wavelengths for minimum reflection at two regions that have different thickness d on the substrate – in well and out of well, by fitting raw data to a parabolic minimum and converted to height in nanometers using eq. 2b, experimentally verified the theoretical red shift of the wavelength corresponding to the thickness increase. RIS also quantitatively measured the height of the OTS coating to be approximately 2.3nm, depicted in Figure 8c, in excellent agreement with literature value for OTS monolayer (Silberzan et.al., 1991) and with what we measured using a spectroscopic ellipsometer. Signal to noise ratios and reproducibility indicate that this implementation of RIS is sensitive to less than 2 Angstrom changes in adsorbed material.

Functionalization chemistry in the reaction wells was carried out as follows. The hydrophilicity-patterned substrates were silanized with 3-aminopropyltriethoxysilane (APTES)

followed by baking in a drying oven. Sulfo-NHS-biotin was then used to link the streptavidin to the wells. Biotin modified probe DNA was attached to the streptavidin. Exposure of the wells to 10 picomoles of complementary 15 base oligonucloetides of DNA resulted in 0.4nm average addition of material or ~8% of a dense target monolayer, corresponding to binding of about 40 femtomoles of target DNAs (Lu et.al.,2004).

Summary

We have developed a new sensing technique, RIS, which is based on removal of the destructive interference in the reflected intensity from an anti-reflection coated silicon substrate. We use a wavelength scanning version of the method that provides quantitative data on surface topology and amount of target binding. The ability to determine the wavelength at which the reflectivity minimum is observed limits the method and we have theoretically estimated the contributions of nonmonochromaticity, angular divergence and substrate roughness. In principle, it is possible to detect adsorption without wavelength scanning simply by increases in reflectivity from the substrate surface but recovering quantitative topology in that case is complicated. We patterned the silicon substrate surface by hydro-affinity design to make microarrayed reaction wells for parallel detection and developed simple biofunctionalization chemistry to attach probes onto the sensing surface. Successful detection of picomole quantities of DNA oligonucleotides has been demonstrated.

Reference

Born, M.; Wolf, E. *Principles of optics*, 5th ed.; Pergamon Press: Oxford, New York, Toronto, Sydney & Braunschweig, 1975.

Chan, S.; Li, Y.; Rothberg, L. J.; Miller, B. L.; Fauchet, P. M. *Mater. Sci. Eng., C-biomimetic and Supramolecular Systems.* **2001**, 15, 277–282.

Chee, M.; Yang, R.; Hubbel, E.; Berno, A.; Huang, X. C.; Stern, D.; Winkler, J.; Lockhart, D. J.; Morris, M. S.; Fodor, S. P. A. *Science* **1996,** 274, 610–614.

Cooper, M. A. *Nat. Rev. Drug Discov.* **2002**, 1, 515-528

Iyer, V. R.; Eisen, M. B.; Ross, D. T.; Schuler, G.; Moore, T.; Lee, J. C. F.; Trent, J. M.; Staudt, L. M.; Hudson Jr., J.; Boguski, M. S.; Lashkari, D.; Shalon, D.; Botstein, D.; Brown, P. O. *Science* **1999**, 283, 83-87.

Jenison, R.; Yang, S.; Haeberli, A.; Polisky, B. *Nat. Biotechnol.* **2000**, 19, 62–65.

Jin, G.; Tengvall, P.; Lundstrom, I.; Arwin, H. *Anal. Biochem.* **1995**, 232, 69–72.

Knoll, W. *Annu. Rev. Phys. Chem.* **1998**, 49, 569–638.

Landry, J. P.; Zhu, X. D. *Opt Lett.* **2004**, 29, 581-583.

Lin, V. S. Y.; Motesharei, K.; Dancil, K. P. S.; Sailor, M. J.; Ghadiri, M. R. *Science.* **1997**, 278, 840–843.

Lu, J.; Strohsahl, K. M.; Miller, B. L.; Rothberg, L. J. *Anal. Chem.* **2004**, 76, 4416-4420.

Nelson, B. P.; Grimsrud, T. E.; Liles, M. R.; Goodman, R. M.; Corn, R. M. *Anal. Chem.* **2001**, 73, 1-7.

Pan, S.; Rothberg, L. J. *Nano. Lett.* **2003**, 3, 811–814.

Silberzan, P.; Léger, L.; Ausserré, D.; Benattar, J. J. *Langmuir* **1991**, 7, 1647–1651.